Materials and Design 55 (2014) 851–856

Contents lists available at ScienceDirect

Materials and Design

journal homepage: www.elsevier.com/locate/matdes

Analysis on the mechanical strength of WC-Co cemented carbides under uniaxial and biaxial bending

Y. Torres [a], R. Bermejo [b,*], F.J. Gotor [c], E. Chicardi [c], L. Llanes [d]

[a] Dpto. de Ingeniería Mecánica y de los Materiales, E.T.S. de Ingeniería, Universidad de Sevilla, Avda. Camino de los Descubrimientos s/n, 41092 Sevilla, Spain
[b] Institut fuer Struktur- und Funktionskeramik, Montanuniversitaet Leoben, Peter-Tunner Strasse 5, 8700 Leoben, Austria
[c] Instituto de Ciencia de Materiales de Sevilla (US-CSIC), Av. Américo Vespucio 49, 41092 Sevilla, Spain
[d] CIEFMA – Dpto. Ciencia de los Materiales e Ing. Metalúrgica, ETSEIB, Universitat Politècnica de Catalunya, Av. Diagonal 647, 08028 Barcelona, Spain

ARTICLE INFO

Article history:
Received 21 August 2013
Accepted 19 October 2013
Available online 30 October 2013

Keywords:
Cemented carbide
Mechanical strength
Weibull statistics
Ball-on-three-balls

ABSTRACT

The mechanical strength of three WC-Co grades was determined and compared under uniaxial and biaxial bending. Uniaxial four-point bending was conducted on bar-shaped specimens; biaxial testing was performed on discs using the ball-on-three-balls (B3B) method. Strength results were analysed within the frame of the Weibull theory. Differences in characteristic strength between uniaxial and biaxial bending were explained as an effect of the effective surface tested in each case. A higher Weibull modulus was obtained in one grade, independent of the testing method, which was related to its higher fracture toughness. The use and validity of the B3B biaxial test to determine the strength distribution of cemented carbides is discussed.

1. Introduction

As for other high strength brittle materials, cemented carbides show defect controlling fracture strength, which is associated with the size of the largest (or critical) defect in the material, and this can differ from specimen to specimen (or component to component) [1–3]. The type of intrinsic defects in these materials ranges from pores to non-metallic inclusions, as well as abnormally large carbides or binderless carbide agglomerates, among other microstructural heterogeneities [4–9]. Therefore, strength cannot be described uniquely by a single number, but as a distribution function (related to the defect size distribution), where a probability of failure can be defined as the probability that fracture occurs at a stress equal to or lower than a given value [10,11]. For cemented carbides, as for many brittle materials, an homogeneous crack-size frequency density function $g(a)$ of the form $g \propto a^{-p}$ [10,12,13], with p being a material constant, can be assumed which leads to the well-known probability function (Weibull statistics) [14]:

$$P_f(\sigma, V) = 1 - \exp\left[-\frac{V}{V_0}\left(\frac{\sigma}{\sigma_0}\right)^m\right], \quad (1)$$

where the Weibull modulus, m, describes the scatter of the strength data (with $m = 2(p-1)$), and the characteristic strength, σ_0, is the stress at which, for specimens of volume $V = V_0$, the failure probability is: $P_f(\sigma_0, V_0) = 1 - \exp(-1) \approx 63\%$. The probability of failure increases with the magnitude of the load (i.e. σ) and with the size of the specimens (i.e. V). The size effect on strength is the most prominent consequence of the statistical behaviour of strength in brittle materials. That is, large specimens have higher probability of failure than smaller specimens, under the same applied load. The so-called effective surface or effective volume of a component, i.e. region under tensile applied stress, is given by the integration of the stress field over the surface (or volume) according to [11]:

$$S_{\text{eff}} = \int_{\sigma>0}\left(\frac{\sigma(\vec{r})}{\sigma_r}\right)^m dS, \quad (2)$$

$$V_{\text{eff}} = \int_{\sigma>0}\left(\frac{\sigma(\vec{r})}{\sigma_r}\right)^m dV, \quad (3)$$

where σ_r is an arbitrary reference stress (generally the maximum in the stress field). The integration is done only over surface (or volume) elements where the stress $\sigma(\vec{r})$ is positive (tensile). For simple cases, e.g. the stress field in a bending specimen, the calculation of the integral in Eqs. (2) and (3) can be made analytically [15]. But in general, and especially in the case of components, a numerical solution is necessary.

Recent work showed that the size of cemented carbide specimens tested can be very significant on determining the tensile strength [16]; the microstructural features originating the failure might differ depending on the size of the specimen (i.e. tested volume of material). This is particular relevant when results of specimen characterization are to be extrapolated to real components of different shape and size.

* Corresponding author.
E-mail address: raul.bermejo@unileoben.ac.at (R. Bermejo).

0261-3069/$ - see front matter © 2013 Elsevier Ltd. All rights reserved.
http://dx.doi.org/10.1016/j.matdes.2013.10.051

The experimental characterization of strength using standard approaches such as three- or four-point bending requires a relatively large number of specimens as well as sample preparation (e.g. cutting, grinding, polishing, edge chamfering, etc.). In addition, the preparation of samples (e.g. bending bars) may modify the surface to be tested, thus introducing flaw populations which may mask the inherent strength distribution of the material itself. Furthermore, strength measurement uncertainties (MU) associated with the testing procedure (e.g. inaccurate positioning of the specimens, uneven contact and transfer of load, friction, etc.) can lead to underestimation of the Weibull parameters [17]. This can be very significant in the case of brittle materials with a relatively high Weibull modulus, where such large MU may be in the range of the scatter of the strength.

In this work, strength of three microstructurally different WC-Co cemented carbides is assessed by implementing uniaxial and biaxial bending methods. Uniaxial testing is conducted under four-point bending with two different spans and biaxial testing is performed using the ball-on-three-balls (B3B) methodology. The effect of specimen size on strength is investigated comparing uniaxial and biaxial bending. The suitability of the B3B method is confirmed as alternative to uniaxial bending tests for mechanical characterization of cemented carbides, and proposed for testing in different environments (e.g. humidity and temperature [18,19]).

2. Materials and methods

2.1. Material of study

The materials studied were plain WC-Co cemented carbides provided by DURIT Metalurgia Portuguesa do Tungsténio, Lda. Three grades corresponding to different combinations of carbide grain size (d_{WC}) and cobalt volume fraction (V_{Co}) were investigated (referred to as 16F, 16M and 27C). The designations, compositions, and key microstructural parameters of each grade can be found in [20]. Mean carbide grain size was determined by image analysis using scanning electron microscopy (SEM) micrographs taken from polished and etched surfaces, resulting in d_{WC} = 0.50, 1.06 and 1.66 μm for the 16F, 16M and 27C grades, respectively. Values for cobalt binder thickness (λ_{Co}) and carbide contiguity (C_{WC}) were estimated from best-fit equations, attained after compilation and analysis of data published in a large number of literature studies, on the basis of empirical relationships given by Roebuck and Almond [21], but extending them to include carbide size influence [6]. Values of λ_{Co} = 0.25, 0.30 and 0.76 μm, and C_{WC} = 0.61, 0.32 and 0.18, were estimated for the 16F, 16M and 27C grades, respectively.

2.2. Determination of mechanical strength

2.2.1. Uniaxial bending

Four-point bending (4PB) tests were performed with a fully articulated test jig with two different outer (40 and 20 mm) and inner spans (20 and 10 mm). Tests were carried out at room temperature, under load control using an electro-mechanic testing machine (Model 5505, Instron Ltd.) with a load cell of 100 kN, at a testing rate of 100 N/s. Prismatic bar-shape specimens with dimension (45 × 4 × 3 mm) were loaded until fracture. At least ten samples were evaluated for each grade and test condition. The strength was calculated from the maximum load at fracture as [22]:

$$\sigma_{max} = \frac{3F(s_0 - s_i)}{2bh^2}, \tag{4}$$

where F is the load at fracture, s_0 and s_i are the outer and inner spans, b is the specimen width and h is the specimen height.

2.2.2. Biaxial bending

The biaxial flexural strength was measured using the ball on three balls (B3B) test [23–25], where a disc specimen is supported on three balls and loaded symmetrically by a fourth ball (Fig. 1a). In this loading situation, the three-point support guarantees well-defined three point contacts (see Fig. 1b). At the midpoint of the disc surface opposite to the loading ball a biaxial tensile stress state exists, which is used for the biaxial strength testing. This test has been recognised to be very tolerant for some out of flatness of the disc and also for other small geometries or some misalignment [24]. Furthermore, friction is recognised to be much smaller than in the commonly used bending tests. For these reasons, the B3B-test can also be used in as-sintered and small specimens. Details about the test can be found elsewhere [24]. In our case all four balls had a diameter of 3 mm. The tensile loaded surfaces of the B3B specimens (disks of 0.7–1.5 mm in thickness and 13 mm in diameter) were carefully grounded and polished to 3 μm finish to reach the same surface quality. The biaxial flexural test was carried out using an electromechanic universal testing machine (Model 5505, Instron Ltd.). A pre-load of 10 N was applied to hold the specimen between the four balls. The tests were conducted under load control at a rate of 100 N/s at room temperature (relative humidity of 35 ± 2 % at 25 ± 1 °C). The load was increased until fracture and the fracture load, F, was used to calculate the maximum tensile biaxial stress in the specimen at the moment of fracture. At least 10 specimens were tested for each cemented carbide grade. For an elastically isotropic material the maximum stress σ_{max} corresponding to the fracture load can be calculated as follows:

$$\sigma_{max} = f \cdot \frac{F}{t^2}, \tag{5}$$

where t is the thickness of the disc and f a dimensionless factor, which depends on the geometry of the specimen and the balls, the Poisson's ratio of the tested material and details of the load transfer from the jig into the specimen [23]. The factor f was calculated for each geometry using an applet at Ref. [26]. For the specimens of study (with thickness ranging between 1.5 mm and 0.7 mm) the factor f ranged between 1.1 and 1.5.

The corresponding stress distribution in the disc during biaxial loading is shown in Fig. 1b. The maximal stress is located in the centre of the three balls. It can be inferred from the referred figure that the central region, i.e. approx. 1/20 of the specimen dimension, is stressed with more than 90% of the maximal stress. Therefore, localised strength measurements can be performed. We draw the attention of the reader that both the effective surface and

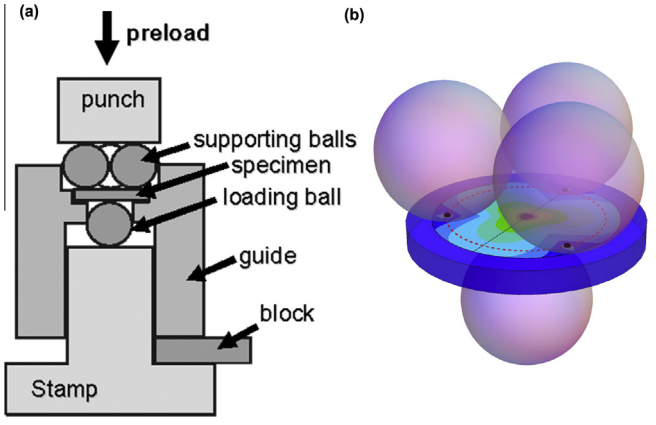

Fig. 1. (a) Schematic of the ball-on-three-balls testing jig; (b) stress distribution in a plate during biaxial loading. The maximal stress is concentrated in the centre of the specimen surface.

volume in the B3B configuration are much smaller than under uniaxial bending.

3. Results and discussion

3.1. Strength distribution: effect of testing configuration

Fig. 2 represents the strength distribution in a Weibull diagram corresponding to the three cemented carbide grades investigated (16F, 16M and 27C), tested under four-point bending with 20–10 mm and 40–20 mm spans and using the ball-on-three-balls method. The failure stress, σ_f, (calculated for every specimen according to Eqs. (4) and (5)) is represented versus the probability of failure, P_f, for the specimens tested. It can be inferred that the failure stress values follow a Weibull distribution, which is associated with the flaw size distribution in the sample (the critical flaw sizes of the samples will be assessed later). The Weibull parameters, σ_0 and m, for all strength distributions were calculated according to the standard EN 843-5 [27]:

$$\ln\ln\left(\frac{1}{1-P_f}\right) = m\cdot\ln\sigma_f - m\cdot\ln\sigma_0, \tag{6}$$

The broken lines in Fig. 2 represent the best fit of the strength data according to Eq. (6) using the maximum likelihood method. The corresponding Weibull parameters (with the 90% confidence interval) for each grade and testing configurations are given in Table 1. The 90% confidence interval for the measured values represents the range where the true Weibull parameters (from the parent distribution) can be found with a 90% probability and reflects the influence of the sampling procedure. The fracture toughness is also given as determined elsewhere [28].

In all three materials an effect of the testing configuration can be observed, especially when comparing uniaxial (4PB) with biaxial (B3B) testing (see Table 1). In the case of biaxial bending higher failure stress values are measured in all three materials. Despite the small number of specimens tested, an effect of the sample tested (effective surface or effective volume) can be clearly seen, which can be explained according to Weibull theory, where the probability of failure increases with the size of the specimen. In our case, the volume of material tested is very different when comparing uniaxial with biaxial testing. Thus, the strength in both cases can be related based on the effective surface S_{eff} (or effective volume V_{eff}) tested in both configurations, according to [10,11]:

$$\sigma^m S_{eff} = \sigma_0^m S_0, \tag{7}$$

and

$$\sigma^m V_{eff} = \sigma_0^m V_0, \tag{8}$$

where the effective surface and volume are calculated with Eqs. (2) and (3) respectively. In the uniaxial bending case, S_{eff} and V_{eff} can be estimated analytically according to [15] as follows:

$$S_{eff} = [h + b(m+1)]\frac{(s_0 + s_i m)}{(1+m)^2}, \tag{9}$$

$$V_{eff} = [bh/2]\frac{(s_0 + s_i m)}{(1+m)^2}, \tag{10}$$

where b is the specimen width, h is the specimen thickness, s_0 and s_i are the outer and inner spans respectively, and m is the Weibull modulus. For the case of biaxial loading using the B3B test S_{eff}

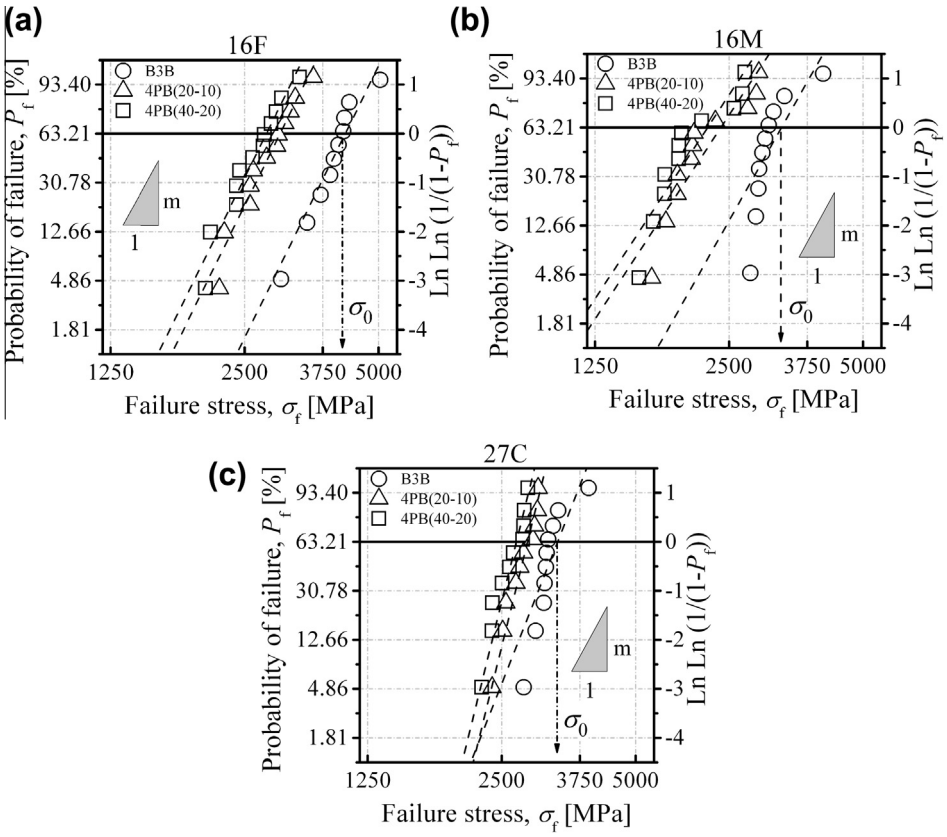

Fig. 2. Failure stress, σ_f, versus the probability of failure, P_f, for (a) 16F, (b) 16M, and (c) 27C samples tested under uniaxial four-point bending (4PB) using 20–10 mm and 40–20 mm spans and under biaxial bending (B3B-test). The broken lines represent the best fit of the strength data according to Eq. (6).

Table 1
Weibull parameters estimated under uniaxial and biaxial bending for three different cemented carbide grades (i.e. 16F, 16M and 27C). The values in brackets represent the 90% confidence interval. Fracture toughness is also given as determined elsewhere [28].

Grade	K_{Ic} [28] (MPa m$^{1/2}$)	Weibull parameters					
		Uniaxial (four-point bending)				Biaxial (ball on three balls)	
		Spans 40 and 20 mm		Spans 20 and 10 mm			
		σ_0 (MPa)	m	σ_0 (MPa)	m	σ_0 (MPa)	m
16F	9.2 ± 0.2	2799 [2605–3012]	8 [5–11]	3004 [2796–3233]	8 [5–11]	4208 [3888–4567]	8 [4–11]
16M	10.5 ± 0.2	2238 [2010–2500]	6 [3–8]	2397 [2151–2681]	6 [3–7]	3281 [3012–3585]	7 [4–10]
27C	14.7 ± 0.2	2699 [2591–2815]	16 [9–21]	2859 [2746–2980]	16 [9–21]	3341 [3133–3571]	10 [6–13]

and V_{eff} were calculated according to Eqs. (2) and (3) with finite element commercial software available at [26]. It is important to observe that both S_{eff} and V_{eff} depend on the Weibull modulus (see Eqs. (2) and (3)). In addition, since a multiaxial stress state exists for the B3B, the calculation of $\sigma(\vec{r})$ requires an equivalent stress σ_e to be defined. The principle of independent action (PIA) is commonly used to calculate the equivalent stress, and accounts for the action of all principal stresses (σ_I, σ_{II} and σ_{III}) independently [29], as: $\sigma_e = \left(\sigma_I^m + \sigma_{II}^m + \sigma_{III}^m\right)^{1/m}$ defined for tensile stresses.

As a result, an effective surface of ~40 mm^2 and ~20 mm^2 was estimated with Eq. (9) according to Ref. [15] for the four-point bending specimens with 40–20 mm and 20–10 mm spans, respectively. An effective surface ranging from only 0.2 to 0.7 mm^2 was obtained for the specimens tested with B3B [23,26]. In terms of effective volume, a value of ~10 mm^3 and ~5 mm^3 was estimated with Eq. (10) for the 4PB specimens with 40–20 mm and 20–10 mm spans, respectively. An effective volume ranging from 0.005 to 0.03 mm^3 was obtained for the specimens tested with B3B depending on the thickness of the disc specimens [23,26].

In order to explain the size effect associated with the testing configuration the characteristic strength of each grade is represented in Fig. 3 as a function of the effective surface and effective volume. The characteristic strength of the 4PB (40–20 mm) configuration is taken as a reference; the broken lines represent the extrapolation of the 90% confidence interval for σ_0 for different S_{eff} (Fig. 3a1, b1 and c1) and V_{eff} (Fig. 3a2, b2 and c2) respectively. According to Fig. 3 the size effect predicted by the Weibull theory can be clearly seen. An extrapolation of uniaxial results shows a good agreement between uniaxial and biaxial strength, when considering fracture originating defects located at the sample surface (effective surface).

The analysis of the fracture surfaces in terms of origin, size and type of defect, for the three grades of cemented carbides investigated revealed that failure origins were found at or near the surface of the specimens; no fracture origin in the interior of the specimens (far from the surface) was found. Thus, the Weibull extrapolation considering the effective surface represented in Fig. 3a1, b1 and c1 should be considered. As inferred from the referred figure, the Weibull theory can explain the difference in strength between samples tested under uniaxial and biaxial bending for the three cemented carbides investigated. A direct consequence is that the strength distributions obtained under biaxial bending using the B3B method can be ascribed to surface (or sub-surface) defect population in the three cemented carbide grades. This qualifies the B3B method to be used for mechanical characterization of cemented carbides as those investigated in this work.

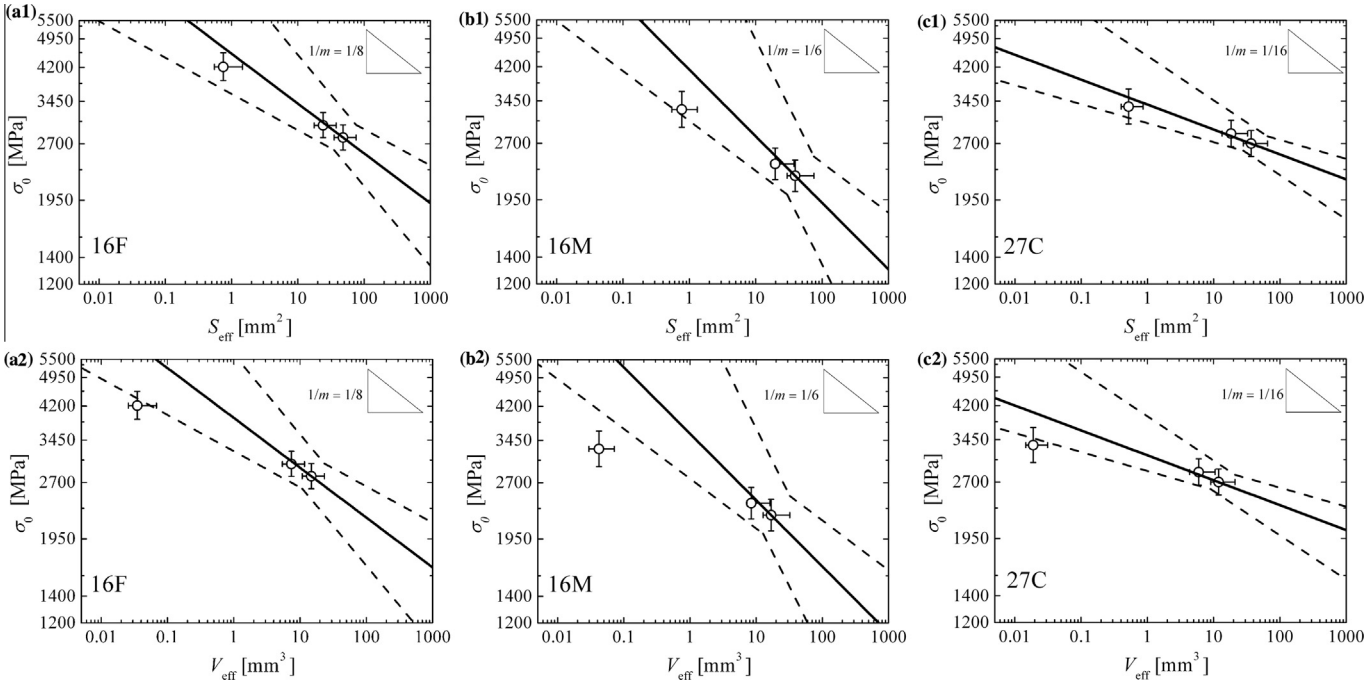

Fig. 3. Characteristic strength of (a) 16F, (b) 16M, and (c) 27C cemented carbide grades as a function of the effective surface (a1, b1 and c1) and effective volume (a2, b2 and c2) according to Weibull theory. The characteristic strength of the 4PB (40–20 mm) samples is taken as reference for the extrapolation. Broken lines (as well error bars in the symbols) describe the 90% confidence intervals.

3.2. Analysis of critical defect size

Based on a linear elastic fracture mechanics (LEFM) approach, the critical defect size (a_c) causing the failure of the uniaxial or biaxial loaded specimens can be estimated based on the failure stress, σ_f (as reported in Table 1), and on the fracture toughness, K_{Ic}, of the material according to the Griffith relation: $K_{Ic} = \sigma_f \cdot Y \cdot (\pi a_c)^{1/2}$. The factor Y can adopt different values depending on the location of the critical flaw. According to [30,31], for the case of internal circular defects Y can be assumed as $2/\pi \approx 0.63$; for small critical surface flaws (semi-circular cracks) Y can be assumed as 0.73; for large critical surface flaws (e.g. scratches) Y can be defined as 1.12; and for sub-surface flaws $Y \approx 0.93$ (due to the subcritical growth up to the surface [30]). In our case, since both surface and sub-surface flaws were found, a factor $Y \approx 1$ was assumed. The estimated mean critical flaw sizes for all three grades under both loading configurations were: (i) 3 μm, 7 μm, and 9 μm under 4PB (40–20 mm), (ii) 3 μm, 6 μm, and 8 μm under 4PB (20–10 mm), and (iii) 2 μm, 3 μm and 6 μm under B3B, for 16F, 16M and 27C, respectively. In general smaller defects could be estimated for the three grades tested under B3B, most likely associated with the lower effective surface (or effective volume) in the sample during testing (i.e. lower probability of encountering large defects). For the case of the B3B, the estimated effective surface calculated above with Eq. (2), i.e. between 0.2 and 0.7 mm^2, corresponds to areas as wide as 400 μm × 500 μm and 700 μm × 1000 μm, respectively. This ensures the validity of the B3B method to sample a representative area of the material tested containing typical sizes of failure initiating defects.

Very interesting is the small difference between 4PB and B3B strength in the 27C grade. This can be associated with the relatively higher K_{Ic} as well as more pronounced R-curve in this grade compared to 16F and 16M (see Torres et al. for more details [32]). As a consequence, although initial defects may have similar size, they can grow sub-critically in the 27C grade up to certain size both under 4PB and B3B configurations. This leads to a certain "homogenization" in size, which can also be inferred from the relatively higher Weibull modulus obtained in the 27C compared to the other two grades (i.e. $m = 16$ for 27C and $m = 8$ for 16F and 16M). According to this result, the B3B method should be able to account for R-curve effects which may be present in cemented carbide grades. Future work will consider the use of B3B to test WC-Co in different environments (e.g. humidity and temperature as employed for other materials [18,19]), where the accuracy of the testing method place a significant role to differentiate strength behaviours under different conditions.

4. Conclusions

Different uniaxial and biaxial strength distributions were measured in three WC-Co grades with different microstructures using the four-point bending (4PB) and ball-on-three-balls (B3B) methods. Characteristic strengths ranging from ~2200 MPa to ~3000 MPa were measured under 4PB, while higher values between ~3300 MPa and ~4200 MPa were obtained under B3B. This could be explained according to the size effect on strength in brittle materials, as predicted by the Weibull theory; extrapolation of 4PB results for effective surface showed good agreement with the B3B experimental values. A higher Weibull modulus was measured in the WC-Co grade with pronounced R-curve under both 4PB and B3B, associated with the subcritical growth of initial defects. The B3B is suggested as alternative method for testing WC-Co cemented carbides, which could be extended to different environments and temperatures.

Acknowledgments

This work was performed within a cooperative effort among DURIT Ibérica, Universidad de Sevilla, Montanuniversität Leoben, Instituto de Ciencia de Materiales de Sevilla and Universitat Politècnica de Catalunya (through funding by the Spanish Ministerio de Economia y Competitividad – Grant MAT 2012-34602). The authors gratefully acknowledge all the above support and stimulating collaboration. Furthermore, the authors want to thank laboratory technician J. Pinto and undergraduate student I. Machuca, for their assistance in mechanical testing.

References

[1] Davidge RW. Mechanical behaviour of ceramics. Cambridge: Cambridge University Press; 1979.
[2] Danzer R. Ceramics: mechanical performance and lifetime prediction. In: Cahn RW, Brook R, editors. Encyclopedia of advanced materials. Oxford: Pergamon Press; 1994. p. 385–98.
[3] Munz D, Fett T. Mechanical properties, failure behaviour, materials selection. Berlin: Springer; 1999.
[4] Fischmeister H. Development and present status of the science and technology of hard materials. In: Viswanadham RK, editor. Proc of ICSHM1 – 1st Int Conf on the Science of Hard Materials. New York: Plenum Press; 1981. p. 1–45.
[5] Morrell R. Fractography of brittle materials. In: NPL, editor. Measurement good practice guide No. 15. Teddington, UK, 1999.
[6] Torres Y. Comportamiento mecánico de carburos cementados WC-Co [PhD Thesis]. Ciencia de los Materiales e Ingeniería Metalúrgica. Barcelona: Universitat Politècnica de Catalunya; 2002.
[7] Coureaux D. Comportamiento mecánico de carburos cementados WC-Co: Influencia de la microestructura en la resistencia a la fractura, la sensibilidad a la fatiga y la tolerancia al daño inducido bajo solicitaciones de contacto [PhD Thesis]. Ciencia de los Materiales e Ingeniería Metalúrgica. Barcelona: Universitat Politècnica de Catalunya; 2012.
[8] Li A, Zhao J, Wang D, Gao X, Tang H. Three-point bending fatigue behavior of WC-Co cemented carbides. Mater Des 2013;45:271–8.
[9] Chicardi E, Torres Y, Córdoba JM, Hvizdoš P, Gotor FJ. Effect of tantalum content on the microstructure and mechanical behavior of cermets based on $(Ti_xTa_{1-x})(C_{0.5}N_{0.5})$ solid solutions. Mater Des 2014;53:435–44.
[10] Danzer R. A general strength distribution function for brittle materials. J Eur Ceram Soc 1992;10:461–72.
[11] Danzer R, Lube T, Supancic P, Damani R. Fracture of advanced ceramics. Adv Eng Mat 2008;10(4):275–98.
[12] Jayatilaka A, Trustrum K. Statistical approach to brittle fracture. J Mater Sci 1977;12:1426–30.
[13] Hunt RA, McCartney LN. A new approach to Weibull's statistical theory of brittle fracture. Int J Fract 1979;15(4):365–75.
[14] Weibull W. A statistical distribution function of wide applicability. J Appl Mech 1951;18:253.
[15] Quinn GD. Weibull strength scaling for standardized rectangular flexure specimens. J Am Ceram Soc 2003;86(3):508–10.
[16] Klünsner T, Wurster S, Supancic P, Ebner R, Jenko M, Glätzle J, et al. Effect of specimen size on the tensile strength of WC-Co hard metal. Acta Mater 2011;59(10):4244–52.
[17] Bermejo R, Supancic P, Danzer R. Influence of measurement uncertainties on the determination of the Weibull distribution. J Eur Ceram Soc 2012;32(2):251–5.
[18] Bermejo R, Supancic P, Aldrian F, Danzer R. Experimental approach to assess the effect of metallization on the strength of functional ceramic components. Scripta Mater 2012;66(8):546–9.
[19] Bermejo R, Supancic P, Krautgasser C, Morrell R, Danzer R. Subcritical crack growth in Low Temperature Co-fired Ceramics under biaxial loading. Eng Fract Mech 2013;100:108–21.
[20] Llanes L, Torres Y, Anglada M. On the fatigue crack growth behavior of WC-Co cemented carbides: kinetics description, microstructural effects and fatigue sensitivity. Acta Mater 2002;50:2381–93.
[21] Roebuck B, Almond EA. Deformation and fracture processes and the physical metallurgy of WC-Co hardmetals. Int Mater Rev 1988;33:90–100.
[22] EN 843-1. Advanced technical ceramics, monolithic ceramics, mechanical properties at room temperature, Part 1: Determination of flexural strength. 1995.
[23] Börger A, Supancic P, Danzer R. The ball on three balls test for strength testing of brittle discs: stress distribution in the disc. J Eur Ceram Soc 2002;22(9–10):1425–36.
[24] Börger A, Supancic P, Danzer R. The ball on three balls test for strength testing of brittle discs: Part II: analysis of possible errors in the strength determination. J Eur Ceram Soc 2004;24(10–11):2917–28.
[25] Danzer R, Harrer W, Supancic P, Lube T, Wang Z, Börger A. The ball on three balls test – strength and failure analysis of different materials. J Eur Ceram Soc 2007;27(2–3):1481–5.

[26] http://www.isfk.at/de/960/ (accessed on 12.02.13).
[27] EN 843-5. Advanced technical ceramics, monolithic ceramics, mechanical properties at room temperature, Part 5: Statistical analysis. 1997.
[28] Torres Y, Casellas D, Anglada M, Llanes L. Fracture toughness evaluation of hardmetals: influence of testing procedure. Int J Refract Met Hard Mater 2001;19(1):27–34.
[29] Freudenthal AM. Statistical approach to brittle fracture. In: Liebowitz H, editor. Fracture, vol. II. New York, London: Academic Press; 1968. p. 591–619.
[30] Danzer R, Reisner G, Schubert H. Der Einfluß von Gradienten in der Defektdichte und Festigkeit auf die Bruchstatistik von spröden Werkstoffen. Zeitschrift für Metallkunde 1992;83:508–17.
[31] Mayrhofer K, Fischer FD. Advances in fracture research. Oxford, Uk: Pergamon Press; 1989.
[32] Torres Y, Bermejo R, Llanes L, Anglada M. Influence of notch radius and *R*-curve behaviour on the fracture toughness evaluation of WC-Co cemented carbides. Eng Fract Mech 2008;75(15):4422–30.